S20-32

219966

N90-19269

ANTENNAS FOR 20/30 GHz AND BEYOND

C. Harry Chen, William C. Wong and S. Jim Hamada
TRW Electronic Systems Group, Antenna Systems Laboratory
Redondo Beach, CA

In the past three decades, NASA has been the prime mover in a series of experimental satellites, which then expanded into the space industry. NASA sponsored the basic research and development and the industry developed and optimized the performance of the systems. This is shown by the development of the space communications technology, in which several NASA programs played significant milestones as shown in Figure 1. Figure 1 also shows that the spaceborne antenna technology trend is moving up into 20/30 GHz and even higher frequency bands.

The advantages of high frequency have long been recognized, i.e. smaller hardware size, lighter weight, higher antenna gain (for the same aperture size), narrower beamwidth (thus better resolution), and broader baseband bandwidth (for the same percentage bandwidth). The challenges to successfully design and develop a spaceborne antenna are also numerous: the design and analysis capability to achieve and assure the high performance; the component/device availability to put a system together; the manufacturing capability to meet the tight tolerances; and the integration and test capability to precisely assemble and align the antenna system and accurately verify the performance. This paper describes how the industry faces these challenges using primarily the Multibeam Antenna (MBA) system of the Advanced Communication Technology Satellite (ACTS) [1] as an example. Even though the technology and the hardware developed in this program are for space communications application, they are applicable to other space applications requiring 20/30 GHz and higher frequency.

ACTS – A Showboat of Ka-Band Technology

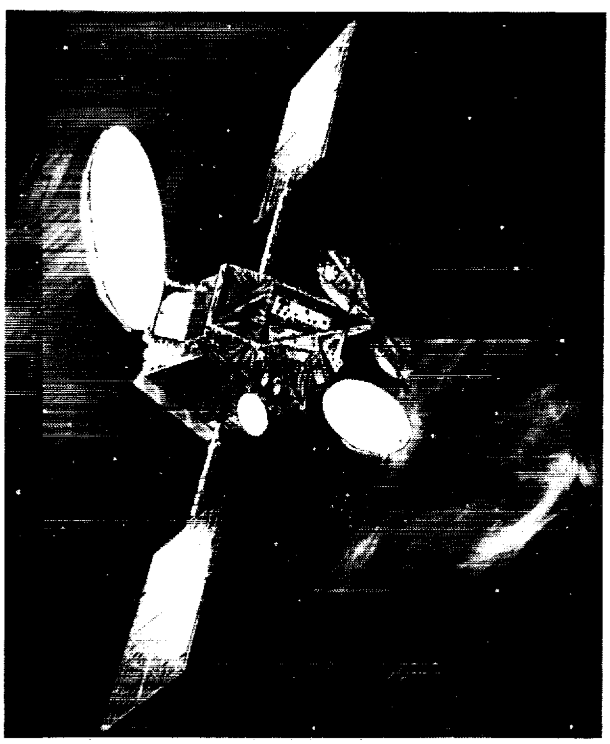

Satellite	Launch	Comments
NASA SYNCOM	1963	First communication satellite at geosynchronous altitude
Intelsat I	1965	C-band
Intelsat II	1967	C-band
Intelsat III	1968	C-band
Intelsat IV	1971	C-band
NASA ATS-6	1974	Demonstrated the full technology and capability of communications satellite
Intelsat IV-A	1975	C-band
NASA CTS	1976	Demonstrated Ku-band technology
Intelsat V	1980	C- & Ku-bands
Intelsat VI	Under construction	C- & Ku-bands
NASA ACTS	1990	To demonstrate Ka-band technology

Figure 1

ORIGINAL PAGE IS OF POOR QUALITY

The ACTS MBA system was designed to demonstrate a spaceborne antenna's capability of producing multiple fixed, scanning and overlapping beams with a single aperture while maintaining good isolation between beams and precise pointing of each beam. The beamwidth is approximately 0.3 degrees with 0.01 degree pointing accuracy. This extremely narrow beamwidth along with the weight and stowage constraints of the Space Shuttle cargo bay dictates that a reasonably large antenna aperture operating at 20/30 GHz must be used. To allow frequency reuse on as many fixed beams (which serve high data rate) as possible, sidelobe roll-off (below -30 dB) and high cross-polarization (also below -30 dB) are of utmost importance as these determine the minimum allowable beam spacing to meet the beam-to-beam isolation requirement. For the overlapping beams (which serve low data rate to scan sectors), the beam-to-beam isolation is attained through cross-polarization and/or time division multiplexing (TDM). The TDM coverage of each scan sector is accomplished by the beam forming network (BFN). The scan spot beams, usable as high data rate fixed beams or low data rate TDM beams, are also connected to the BFN. The ACTS MBA beam coverage and polarization, including 3 fixed beams, 13 scan spot beams and 2 scan sectors, are illustrated in Figure 2. The 3 fixed beams are Cleveland, Atlanta and Tampa. The Cleveland beam also serves as the tracking beam.

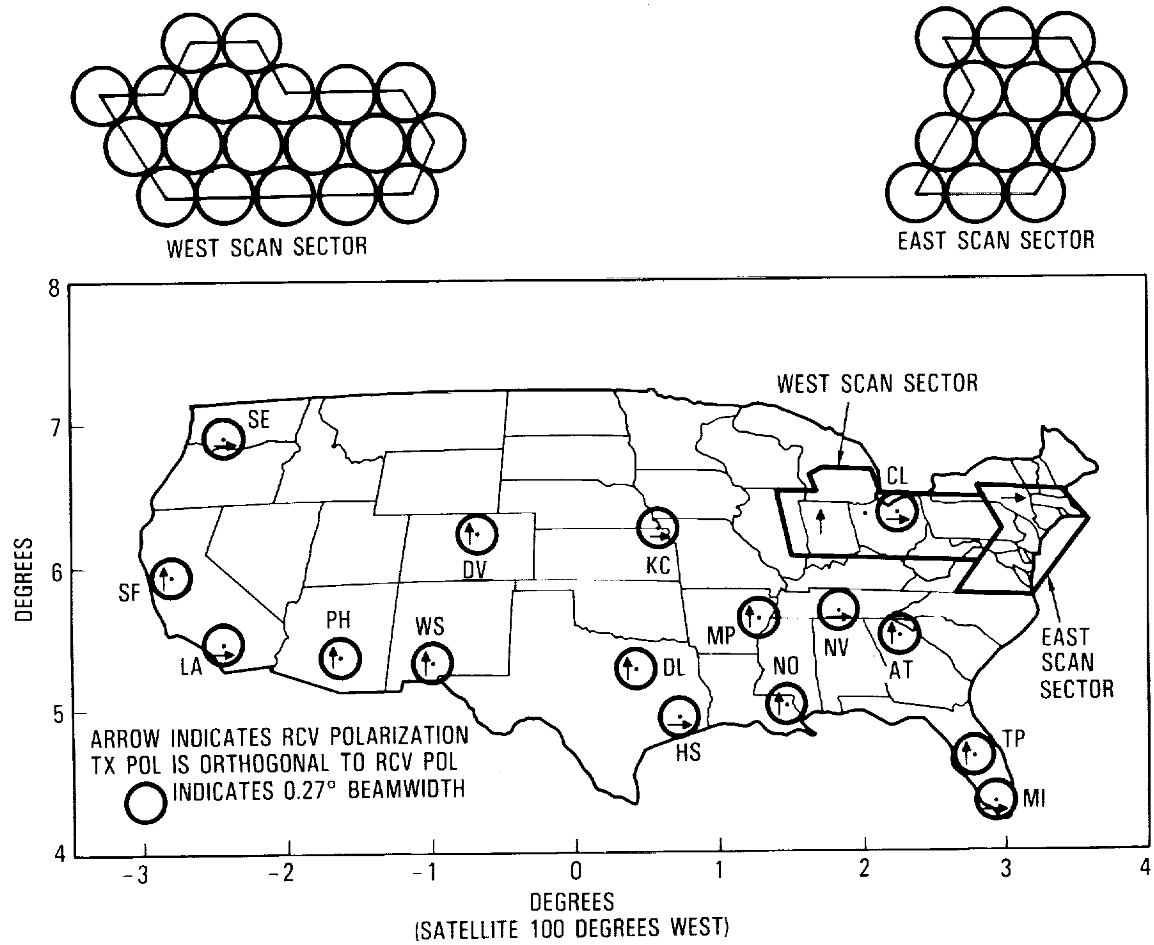

Figure 2

ACTS MULTIBEAM ANTENNA CONFIGURATION

The capabilities that ACTS MBA's are required to demonstrate were never before demanded of a communications satellite antenna, leading to antenna configurations with unprecedented complexity. Both receive and transmit MBA's are offset Cassegrain systems with dual subreflectors in a piggyback arrangement (Figure 1). The Cassegrain system is used to obtain large equivalent F/D, thus minimizing the scan loss. (Some spot beams, e.g. San Francisco, scan as far as 15 half-power beamwidth.) The offset configuration eliminates the gain and sidelobe degradation due to blockage. The front subreflector is gridded, transparent to one sense of polarization and reflective to the orthogonal sense of polarization. The polarization passing through the front subreflector is reflected by the solid back subreflector and passes through the front subreflector again. The polarizer characteristic of the front subreflector enhances the cross-polarization isolation by at least 10 dB between orthogonally polarized beams. To avoid mechanical interference, the focal axes of the two subreflectors are symmetrically displaced from the main reflector axis by an angle of 10 degrees, creating two focal regions for the two feed assemblies and BFN's. The important design parameters of the MBA's are listed in Figure 3.

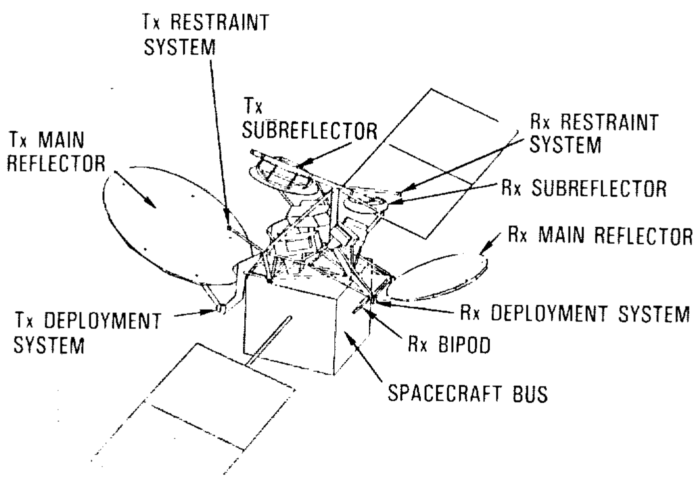

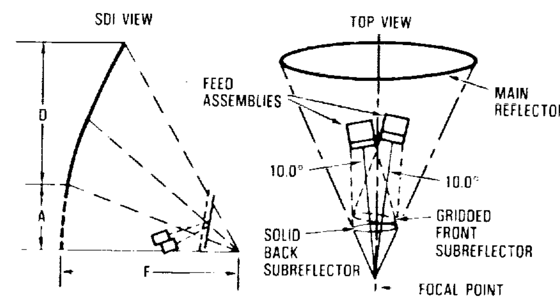

Parameter	ACTS 20 GHz	ACTS 30 GHz	Breadboard (30 GHz)
D (Main reflector diameter) (meters)	3.3	2.2	2.7
A (Offset distance) (inches)	50.0	44.0	56.12
F (Main reflector focal length inches)	132.0	88.0	132.0
Gridded front subreflector			
Focal length (inches)	69.0	44.5	84.0
Magnification factor	2.0	2.0	2.0
Solid back subreflector			
Focal length (inches)	52.4	32.4	66.0
Magnification factor	2.0	2.0	2.0

Figure 3

ORIGINAL PAGE IS OF POOR QUALITY

REFLECTOR SURFACE CONTROL FOR LOW SIDELOBE PERFORMANCE

The deviation of the reflector from the prescribed surface affects both the amplitude and phase distribution in the aperture plane, causing both wide angle sidelobe and near-in sidelobe degradations. This effect is illustrated in Figure 4. With surface distortion, the well-behaved sidelobe structure of concentric rings as observed on the pattern without distortion is disturbed. These patterns were computed for the ACTS breadboard MBA. The pattern with distortion was obtained by incorporating the measured distortion profile of the breadboard reflector (0.0057 inch rms error) into the computation model. The distortion causes the first sidelobe level to degrade from -29 dB to -26 dB, which was later verified by the near-field testing. Traditionally, the surface distortion is characterized by root-mean-square error under the assumption that the distortion is of the random type. In reality, the distortion, closely relating to the manufacturing procedure and the reflector's supporting structure, is deterministic and the distortion profile determines how the sidelobe is degraded. Therefore, in addition to the stringent manufacturing tolerance (4 mils for receive and 6 mils for transmit), the ACTS reflectors are also subject to post-fabrication adjustment to correct the surface anomaly. If the surface distortion analysis based on the measured distortion profile predicts that the particular profile will cause excessive sidelobe degradation, the surface is adjusted.

Sidelobe Degradation Due to Reflector Surface Distortion

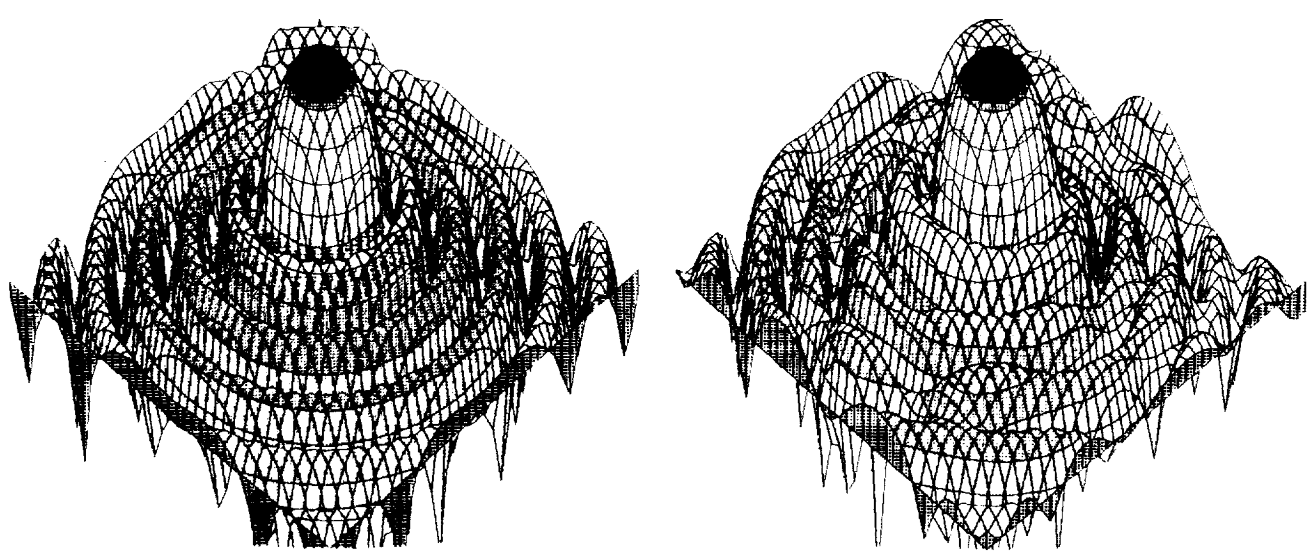

THEORETICAL RADIATION PATTERN WITHOUT REFLECTOR SURFACE DISTORTION

THEORETICAL RADIATION PATTERN WITH REFLECTOR SURFACE DISTORTION

Figure 4

ON-ORBIT THERMAL DISTORTION

On-orbit thermal conditions introduce additional distortion to the reflector surface. The thermal conditions vary from time to time, from day to day and from season to season and thus the thermal distortion effects are time-variant. An example is illustrated in Figure 5 where the sun illuminates the ACTS MBA's at 20:00 hours Eastern Standard Time during winter solstice. The receive antenna is half-shadowed by the subreflectors, resulting in maximum temperature gradient and thus the maximum surface distortion. The transmit antenna, illuminated on the backside in this case, is not very much affected due to the thermal blanket protection. The three-step thermal distortion analysis procedure is summarized in Figure 5. Results obtained from several study cases on the ACTS MBA's [2] show that, without the assistance of an autotracking system, the thermal distortion may cause as high as 0.02 degree pointing error. (Notice that the half-power beamwidth is 0.3 degrees.) The gain degradation may be as high as 0.6 dB.

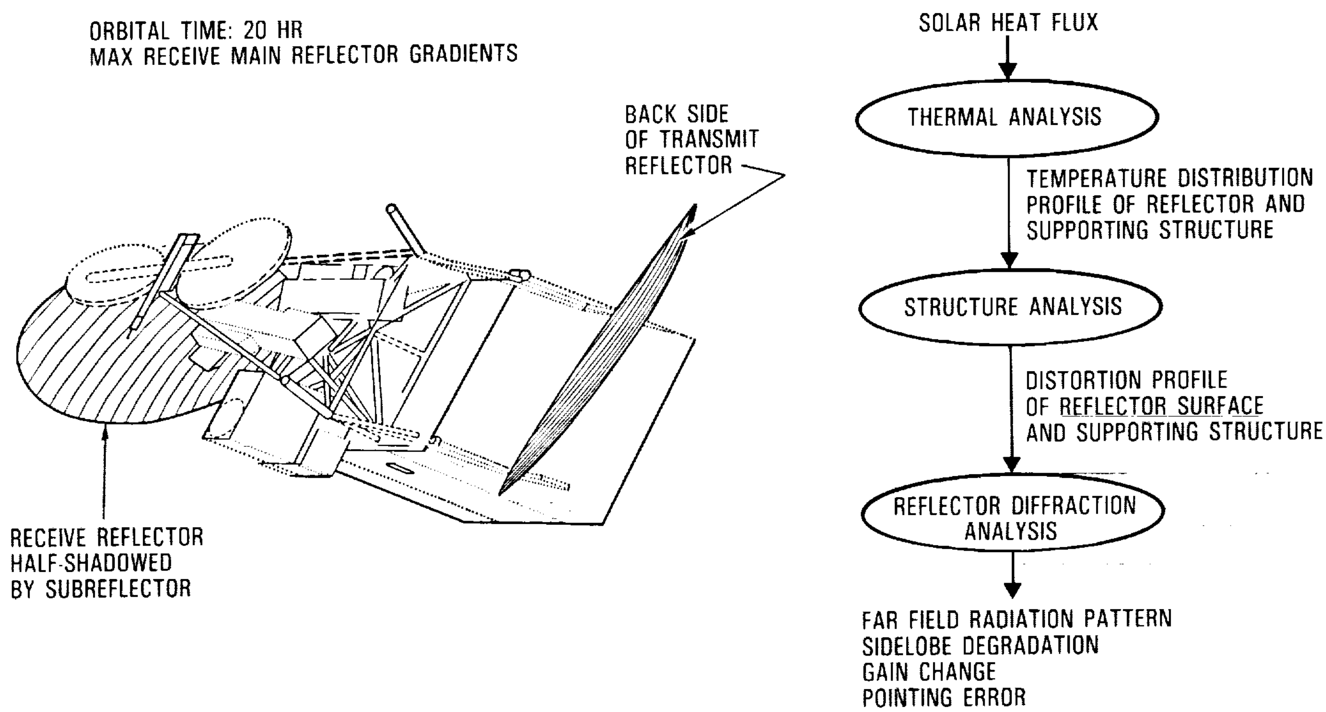

Figure 5

ORIGINAL PAGE IS
OF POOR QUALITY

MULTI-FLARE FEEDHORN

ACTS MBA's use multiflare horns as the primary illuminators [3]. Efficient reflector illumination requires the primary field to be rotationally symmetrical with low sidelobe levels. For maximum gain, the primary field illuminates the reflector with approximately -10 dB edge taper while, for low sidelobe, -17 dB or even higher. Among the three types of feedhorns often used as the primary feeds: dual mode horn (Potter horn), corrugated horn, and multiflare horn, the corrugated horn is most often used due to its broadband performance and good edge taper control. The following table compares the three types of horns. In many applications, the bandwidth requirement excludes using the narrow-band dual mode horns. The major advantage of a multi-flare horn is that it generates radiation patterns similar to that of a corrugated horn (Figure 6) with reasonable bandwidth performance and much simpler mechanical design. The fabrication of the horn throat matching and the grooved walls of a corrugated horn becomes difficult in the millimeter frequency range.

Horn Type	Bandwidth	Impedance Matching	Structure Complexity	Fabrication Cost
Dual-mode horn	Narrow (~4%)	VSWR 1.2:1	Moderate	Moderate
Corrugated horn	Very wide (>30%)	Require throat matching to obtain low return loss	Complicated	High
Multi-flare horn	Wide (~15%)	VSWR 1.07:1 over 20% BW without matching device	Simple	Low

Comparison Between Multiflare Horn and Corrugated Horn

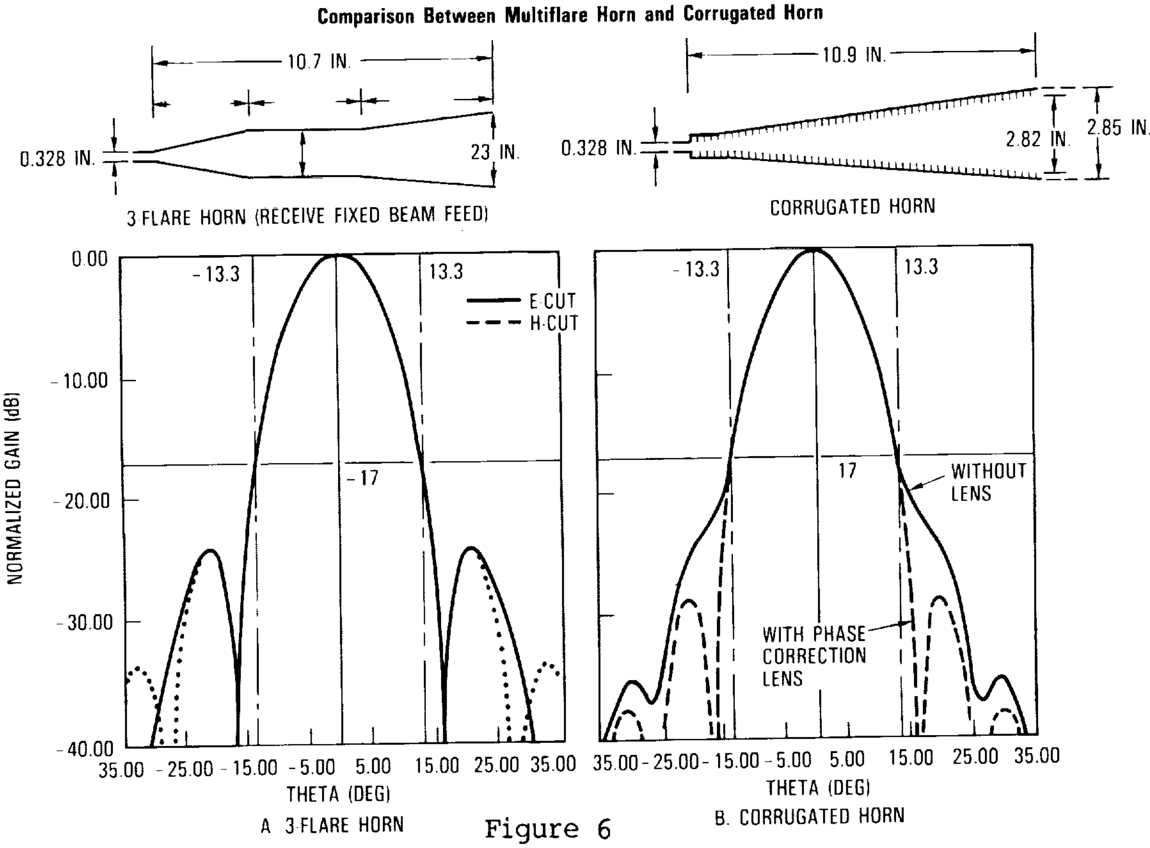

Figure 6

ORIGINAL PAGE IS OF POOR QUALITY

MULTI-FLARE HORN: SUM AND DIFFERENCE MODES

With the use of a tracking mode coupler [4], higher waveguide modes can be excited in a multiflare horn, providing difference patterns for tracking, a more efficient tracking system than the traditional five-horn system. The ACTS MBA autotracking system uses three waveguide modes, TE_{11}, TE_{21} and TM_{01}. The fundamental mode, TE_{11}, serves as a reference signal, the TE_{21} generates an error signal in the azimuth direction, and the TM_{01} generates an error signal in the elevation direction. The two error signals are then biphase-modulated and combined with the reference signal to produce an amplitude modulated signal to be fed into a tracking receiver for autotracking. Theoretical analysis based on mode matching at the flare break to compensate for phase front curvature change [5] and taking into account the differential phase shift of each waveguide mode between flare breaks predicts a multi-flare horn's radiation pattern well, both sum and difference, as shown in Figure 7.

Multiflare Horn Sum (TE_{11}) and Difference (TM_{01}, TE_{21}) Pattern

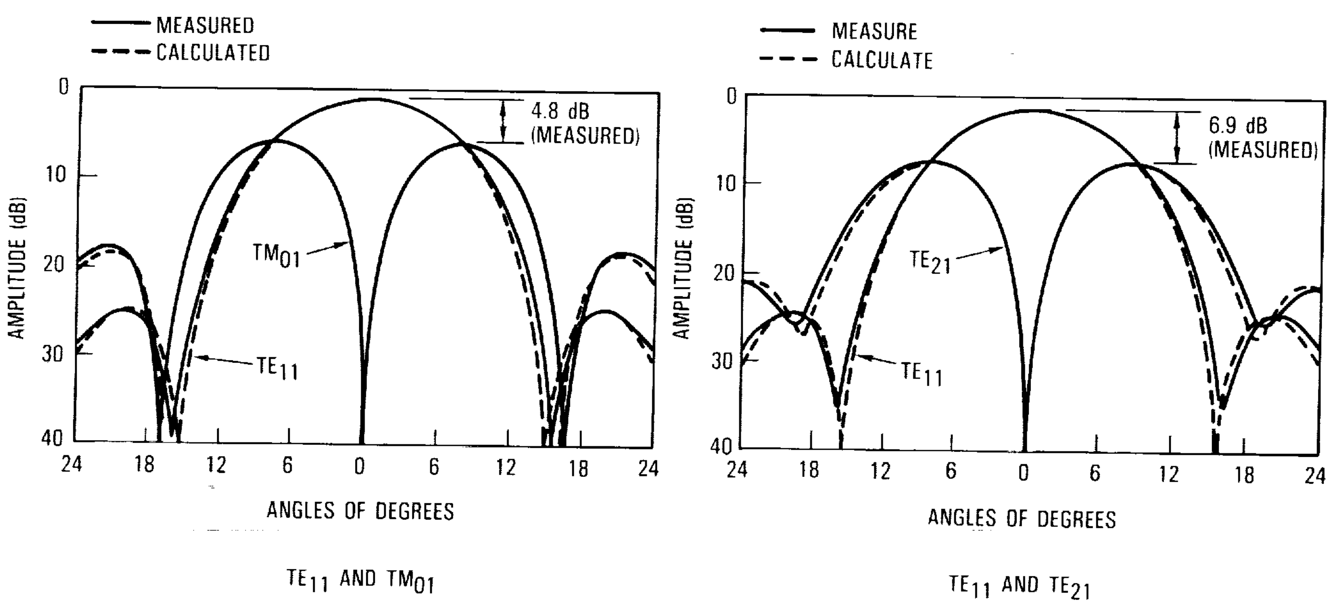

Figure 7

SIDELOBE CANCELLATION

Besides the accurate reflector surface control and the use of an efficient primary radiator with high edge taper, the low sidelobe performance can further be improved using a feed cluster. This is achieved by carefully spacing the feed so that the first sidelobe (of the secondary pattern) of the center feed coincides with half of the main lobe of the adjacent feed and the second sidelobe of the center feed coincides with the first sidelobe of the adjacent feed. Under this condition, the sidlobes of the adjacent feeds are approximately out of phase and will cancel each other with proper amplitude adjustment. Figure 8 demonstrates the improvement on sidelobe level using this technique. The technique was not used on ACTS MBA since the sidelobe level achieved by surface tolerance control and high edge taper is sufficient to meet the system requirement.

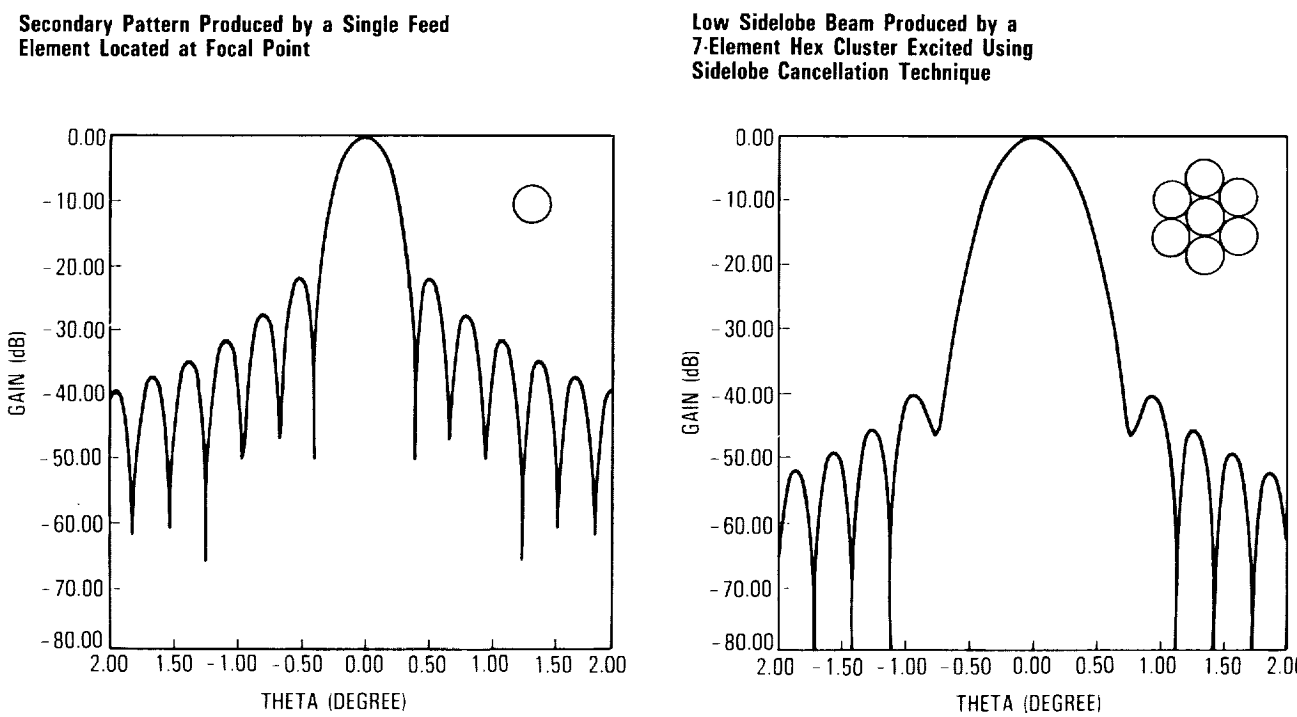

Figure 8

BEAM FORMING NETWORK

The beam scanning capability of a MBA is provided by the Beam Forming Network (BFN). The ACTS MBA has four BFN's, each provides one of two polarizations for either the receive or the transmit antenna. Figure 9 shows the schematic diagram of the horizontally polarized receive BFN. The BFN consists of an RF switch network and redundant control electronics. The RF switch network is formed by a number of latching ferrite switches, a fixed power combiner and interconnecting waveguides. The control electronics include switch drivers and a controller to accept and interpret switching commands. Depending on the switching status of the network, a feed is selected. The scanning is achieved by sequentially selecting different feeds. When scanning within a scan sector, three adjacent feeds (one from each of the groups A, B and C) are selected to form a triplet. By hopping from triplet to triplet, the entire sector is covered. Typical BFN performances are:

Switching Time : less than 0.8 microsecond
Insertion Loss : less than 0.1 dB per switch
Isolation : better than 25 dB per switch

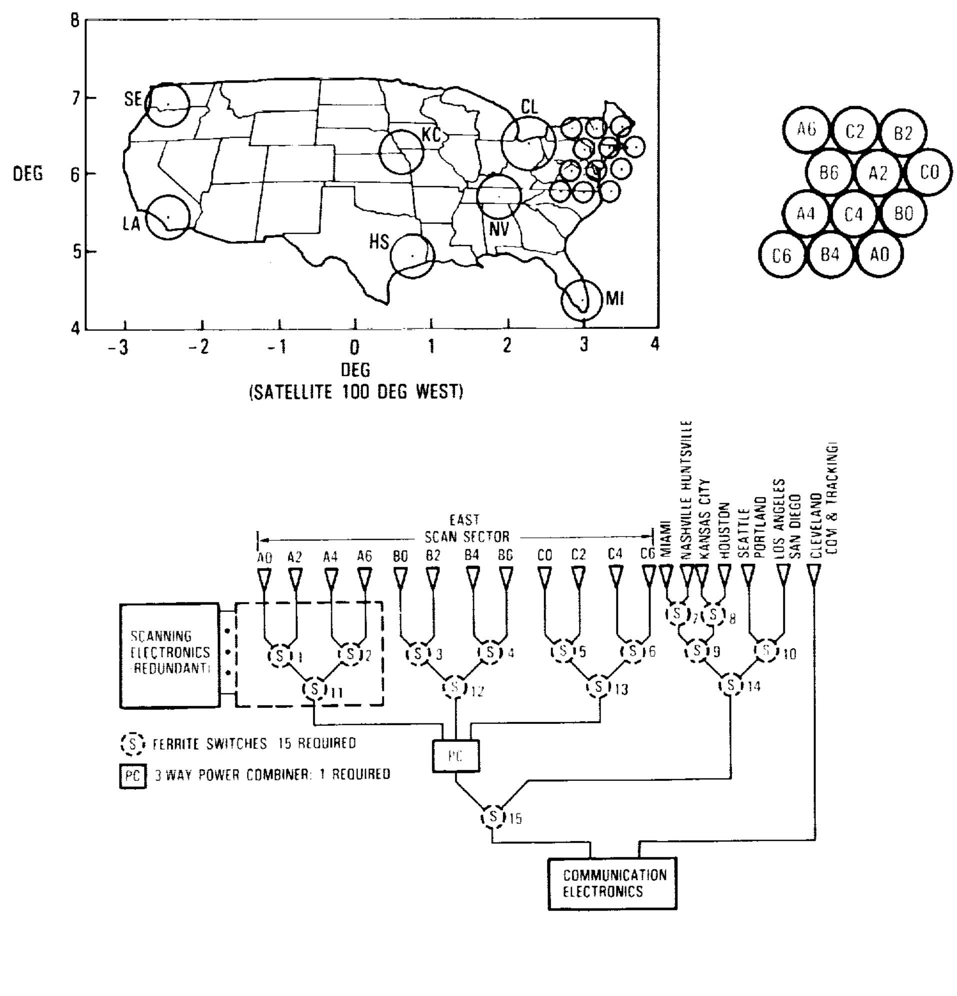

Figure 9

ORIGINAL PAGE IS
OF POOR QUALITY

FEED ASSEMBLY

Figure 10 illustrates the physical implementation of the BFN of Figure 9 and the feed assembly. Notice that the Nashville and Miami horns are not shown to expose the trimode tracking system described in Figure 7. The interconnecting waveguides of BFN were electroformed to achieve the required bending and twisting, as well as low loss. The BFN and the feed horns are enclosed in a graphite fiber reinforced plastic (GFRP) housing to achieve high structural rigidity. The near-zero thermal expansion of the GFRP housing provides feedhorns with positional stability throughout the operational and non-operational environments to meet the pointing accuracy requirement. The feed assemblies, the main reflector, and the subreflectors will have to be aligned precisely with respect to each other during the final assembling of the entire MBA so that all beams will simultaneously point to the designed directions. This is discussed in the figure for near-field testing on ACTS breadboard MBA.

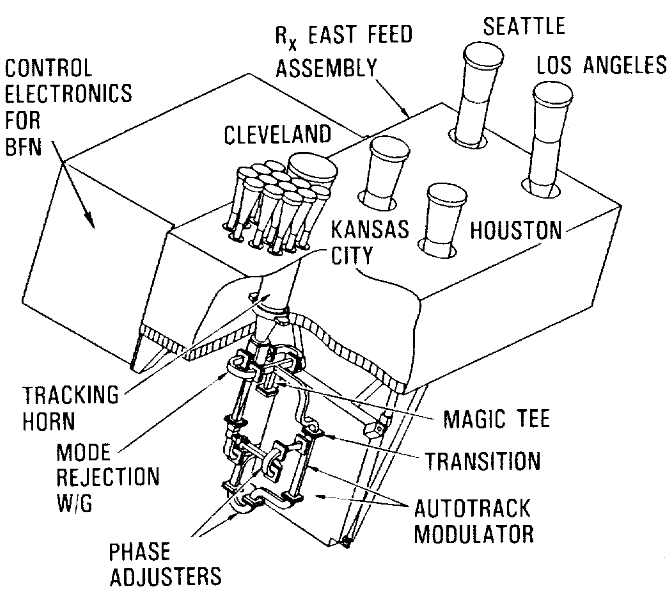

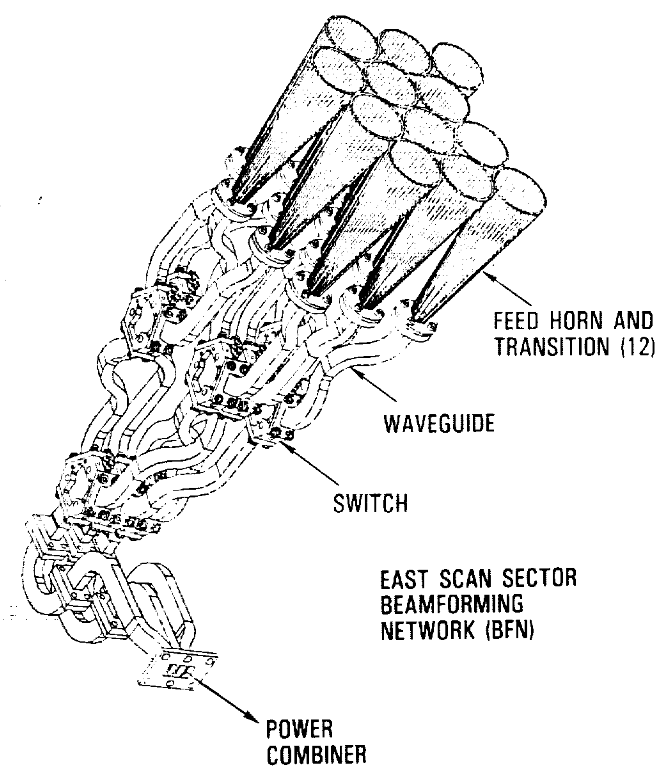

Figure 10

The ability of testing performance and verifying design of mechanically complicated, high-performance antennas such as ACTS MBA's requires the most advanced antenna testing system. The traditional far-field antenna test ranges are outdoor and subject to weather, environmental and security problems. Controlled environmental antenna testing can be performed in an anechoic chamber, but is limited to physically small antennas. Large aperture antenna testing (especially at high frequency) needs a fairly long distance between the source antenna and the AUT (Antenna under Test), and certainly cannot be carried out in an anechoic chamber. For example, testing ACTS 2.2 meter antenna at 30 GHz will require a distance of almost 1000 meters. With the near-field measurement technique, testing large aperture antennas in a controlled environment is possible. In addition, the near-field measurement provides the complete azimuth and elevation radiation patterns, not just a few cuts. Figure 11 shows the ACTS breadboard MBA under near-field testing. As will be described in Figure 12, the near-field range is an integration and test facility, unlike the far-field range - a testing only facility, implying cost and time saving in developing a complicated spaceborne antenna.

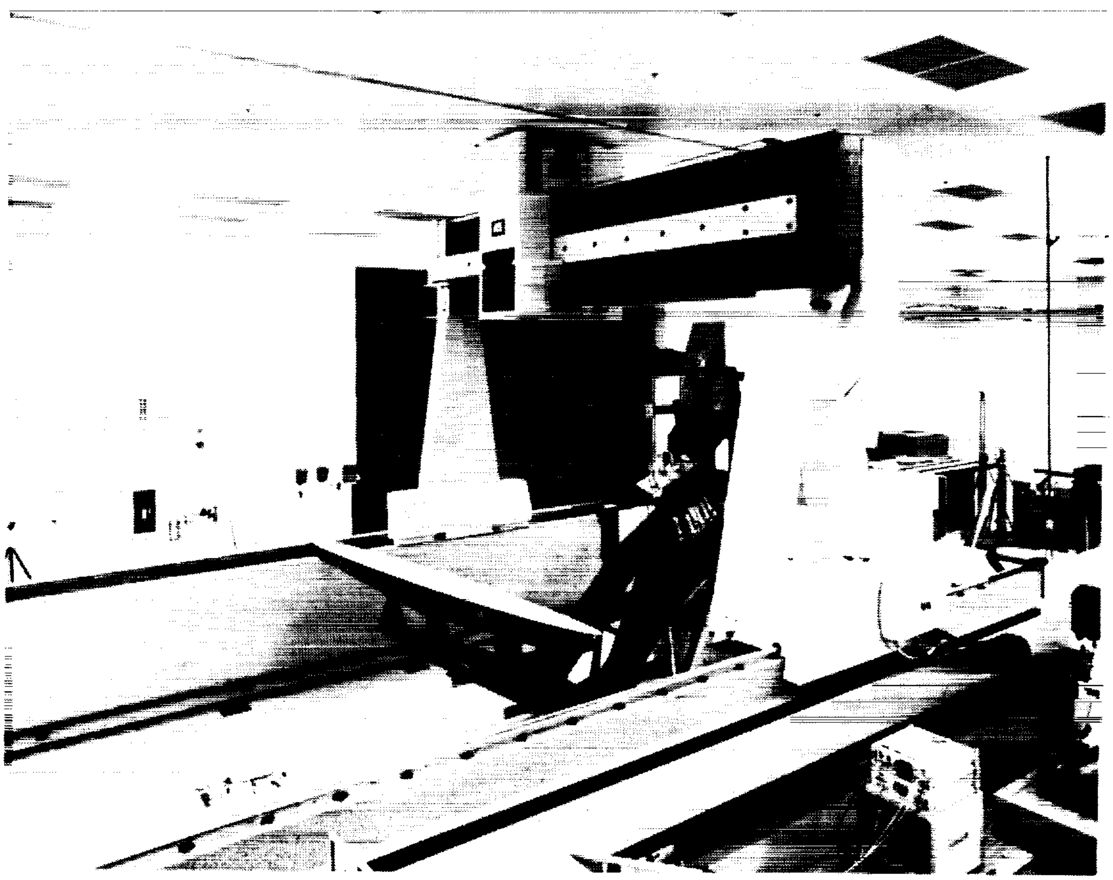

Figure 11

NEAR-FIELD TESTING ON ACTS BREADBOARD MBA

Before the RF test started, the ACTS breadboard MBA was assembled and aligned in the near-field range using the scanner as a precision position measuring system [6]. The RF probe was replaced by a mechanical touching probe. The antenna was aligned with the aid of several tooling balls installed on the MBA at various locations. The ball position as measured by the touching probe was compared to the designed position such that necessary adjustments to the antenna could be made to minimize the difference. The procedure iterated on all tooling balls until the position differences between the measured and the designed were all within tolerance. Assembling and testing the antenna at the same location result in substantial time and cost saving (especially when adjustment is necessary after initial testing), considering the efforts involved in mounting, dismounting and transportation of a complicated antenna.

Figure 12 shows the typical correlation between the calculated and the measured radiation patterns. Other performance parameters assessed include gain, sidelobe level and pointing error [6]. With the above antenna assembly and alignment procedure, a pointing error of less than 0.016 degrees was achieved in one iteration. The breadboard MBA near-field testing verified the ACTS MBA design, developed the flight MBA alignment procedure and provided engineering data to substantiate the flight MBA performance. Most important is that it demonstrates the powerfulness and effectiveness of a near-field test range in developing and testing a complicated antenna system.

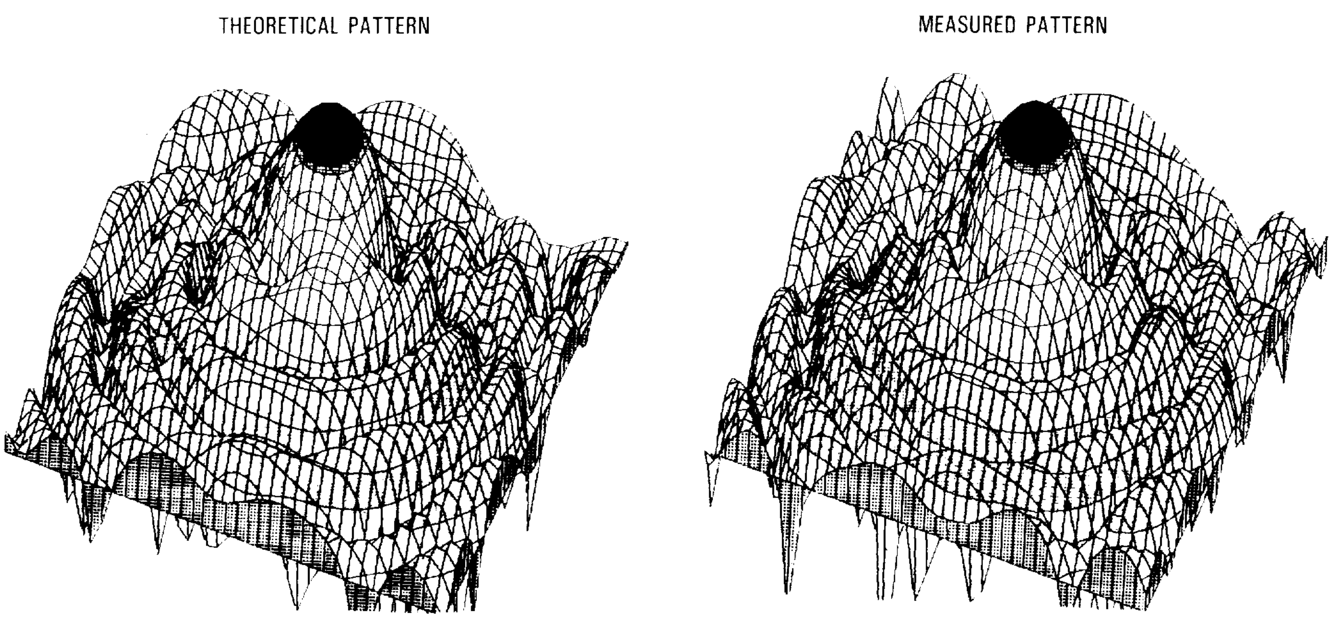

Figure 12

ADAPTIVE MULTIBEAM ANTENNA (AMBA)

An adaptive antenna optimizes the radar or communication system performance (signal-to-noise ratio) via its capability of automatic null steering and notching out interferences in the spatial domain, the frequency and polarization. The interferences may be clutter scatterer returns, natural noise source, unintentional RF interference, or adverse jammers. An adaptive antenna, in the form of a sidelobe canceller, offers an alternate solution to low sidelobe performance requirement.

Even though adaptive antennas are mostly of the phased array type, they can be of the MBA type. An adaptive MBA (Figure 13) [7] is similar to an adaptive phased array pre-weighted with a Butler matrix or a Rotman lens [8] in terms of adapting principle, but less lossy in terms of hardware implementation. Other AMBA advantages include wide bandwidth, large aperture and no grating nulls.

A key component in a adaptive antenna is the weight module which controls amplitude and phase of each feed. The ACTS MBA is not adaptive, nor does the system use any weight module. Nevertheless, the device, developed for other space programs, is available in SHF/EHF* ranges. The AMBA shown in Figure 13 with approximately 150 wavelength reflector is capable of effectively suppressing interference very close to the desired signal.

*Super-high-frequency/extremely high-frequency (SHF/EHF)

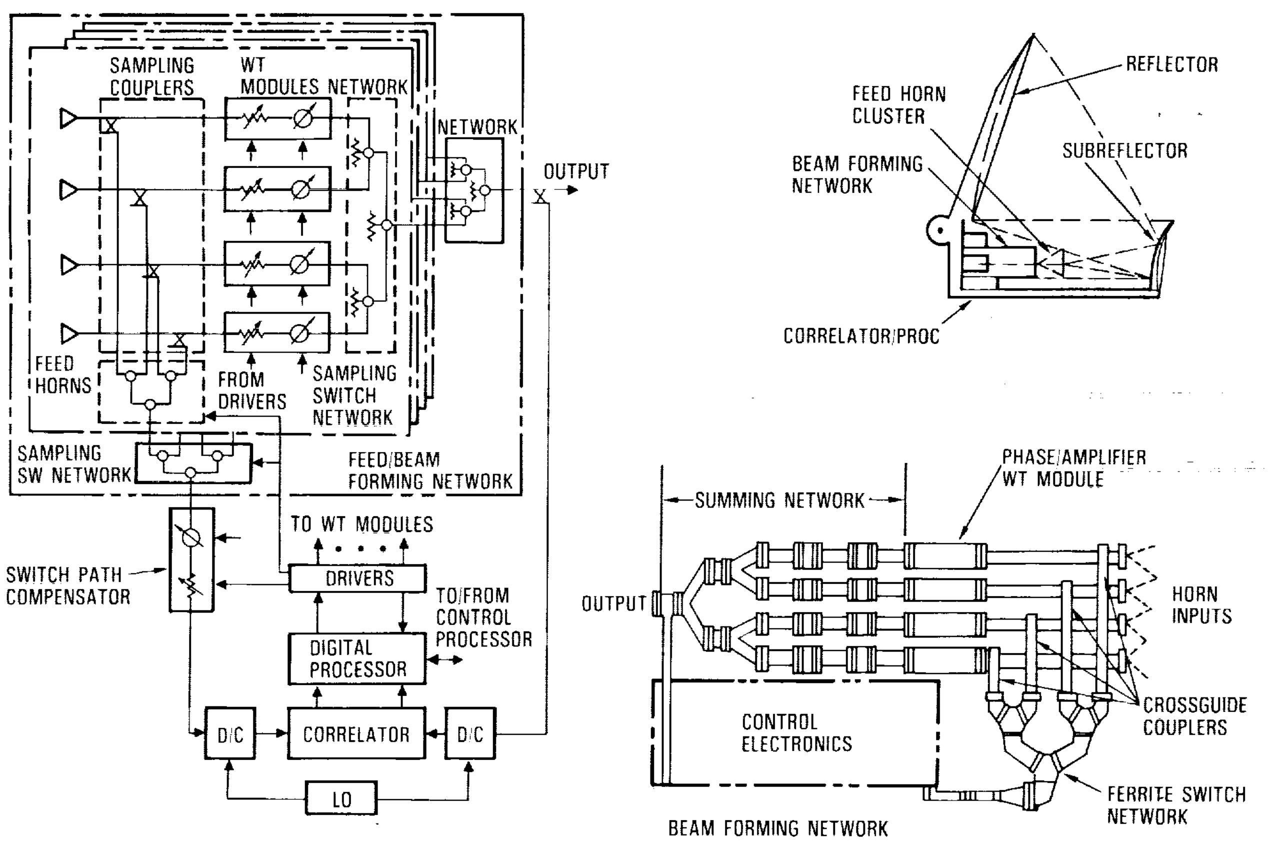

Figure 13

CONCLUSIONS

Antennas of 20/30 GHz and higher frequency, due to the small wavelength, offer unique capabilities for many space applications. With the government-sponsored space programs (such as ACTS) in recent years, the industry has gone through the learning curve of designing and developing high-performance, multi-function antennas in this frequency range. Design and analysis tools (such as the computer modelling used in feedhorn design and reflector surface and thermal distortion analysis) are available. The components/devices (such as BFN's, weight modules, feedhorns and etc.) are space-qualified. The manufacturing procedures (such as reflector surface control) are refined to meet the stringent tolerance accompanying high frequencies. The integration and testing facilities (such as Near-Field range) also advance to facilitate precision assembling and performance verification. These capabilities, essential to the successful design and development of high-frequency spaceborne antennas, shall find more space applications (such as ESGP) than just communications.

REFERENCES

1. Y. Choung, W. Stiles, J. Wu, W.C. Wong, C.H. Chen and K. Oye, "NASA ACTS Multibeam Antenna System," 1986 IEEE Eascon, Washington, D.C., pp 191 - 196.

2. D.Y. Kim, C.H. Chen, K. Oye, W.C. Wong and S.J. Hamada, "Thermal Distortion Analysis on ACTS Multibeam Antenna," 1988 IEEE Antenna and Propagation Symposium Digest, Vol.3, pp. 1310-1313, Syracuse, New York, June 1988.

3. C.H. Chen, Y. Choung and D. Palma, "A Compact Multiflare Horn Design for Spacecraft Reflector Antenna," 1986 IEEE Antenna and Propagation Symposium Digest, Vol.2, pp. 907-910, Philadelphia, Pennsylvania, June 1986.

4. M. Shiau, Y. Choung, C.H. Chen and M. Chen, "NASA ACTS Autotrack Antenna Feed System," 1986 IEEE Antenna and Propagation Symposium Digest, Vol.1, pp. 83-86, Philadelphia, Pennsylvania, June 1986.

5. S.B. Cohn, "Flare Angle Changes in a Horn as Means of Pattern Control," Microwave Journal, Vol. 13, pp 41-46. October 1970.

6. C.H. Chen, W.C. Wong and S.J. Hamada, " Near Field Testing on ACTS Breadboard Multibeam Antenna (MBA)," 1988 IEEE Antenna and Propagation Symposium Digest, Vol.3, pp. 1107-1109, Syracuse, New York, June 1988.

7. P.G. Ingerson, "An Adaptive Nulling MBA Antenna," 1983 IEEE Military Communications Conference, October 31-November 2, 1983, Washington, D.C.

8. J.P Shelton and K.S. Kelleher, "Multiple Beams from Linear Arrays," IRE Transactions on Antennas and Propagation, AP-9, No. 1, P 154, March 1961.